Simulation of the Nuclear-Electromagnetic Cascade Development in an Ionization Spectrometer*

W. V. Jones†
Max-Planck-Institut für Physik und Astrophysik, Institut für Extraterrestrische Physik, 8046 Garching bei München, Germany
(Received 28 April 1969)

A simulation of the longitudinal nuclear-electromagnetic cascade development in an ionization spectrometer has been carried out using a Monte Carlo method. Details of the cascade model and the technique used for the calculations are presented. Calculations have been performed to correspond to an actual spectrometer which was exposed to 10-, 20.5-, and 28-GeV/c incident protons at the Brookhaven Alternating Gradient Synchrotron (AGS). Particle-number distributions predicted by the calculations for different depths in the spectrometer are compared with the measurements. Results predicted by the calculations at higher energies extending up to 1000 GeV are also given. Means and standard deviations of the energy leaking out of the bottom of the spectrometer, as well as the energy dissipated in the form of nuclear disintegrations within the spectrometer, are tabulated for various depths for primary energies ranging between 10 and 1000 GeV. The energy leaking out of the sides of the spectrometer during the AGS measurements is estimated. The calculations show that the sum of particles recorded by the spectrometer increases linearly with energy for events undergoing the first interaction in the top layer of the spectrometer.

I. INTRODUCTION

THE use of an ionization spectrometer to measure the energy of high-energy particles was first introduced in 1957.[1] This device has been used since that time in many major experiments that were designed to study properties of the cosmic radiation.[2–7]

The ionization spectrometer is based on the simple principle that almost all of the energy of a particle incident on an absorber must finally be converted into ionization energy. Although the principle of using such an instrument is simple, its practical use offers some difficulties in correctly interpreting results of energy measurements. The difficulties arise mainly from insufficient understanding of the mixed nuclear-electromagnetic cascading in the absorber. Most of the energy of the incident particle is finally converted into ionization via electromagnetic cascades. It is believed that the electromagnetic cascading process is sufficiently well understood, and these cascades, in fact, have been used extensively and successfully over the past several years to measure the energy of high-energy particles.[8] The cascading of hadrons, on the other hand, is not as well understood because of the present lack of understanding of the basic nuclear interaction. Although the electromagnetic cascade in itself offers few prime problems, the superposition of many such cascades is a much more complicated process. Furthermore, an almost hopeless analytical problem exists when these multiple electromagnetic cascades are superimposed with the cascading hadrons in an ionization spectrometer.

Such problems lend themselves readily to solution by the Monte Carlo method. In addition, the Monte Carlo method offers one of the best means for studying the fluctuations to be expected in problems which are bascially of statistical nature, whereas analytical solutions in most cases only predict average behavior.[9] Investigations, both theoretical[10] and experimental,[11,12] have been performed on the influence of fluctuations on the accuracy of energy determinations made with an ionization spectrometer, but Monte Carlo calculations should greatly enhance our knowledge of the

* Research supported in part by the National Aeronautics and Space Administration, Grant No. NGR 19-001-012, and in part by the National Science Foundation, Grant No. GP/7169.

† Presently at Louisiana State University, Baton Rouge, La. 70803. The author would like to express his appreciation to the Alexander von Humbolt Stiftung for a research stipend at the Max Planck Institut.

[1] N. L. Grigorov, V. S. Murzin, and I. D. Rapoport, Zh. Eksperim. i Teor. Fiz. **34**, 506 (1958) [English transl.: Soviet Phys.—JETP **7**, 348 (1958)].

[2] P. V. Ramana Murthy, B. V. Sreekantan, A. Subramanian, and S. D. Verma, Nucl. Instr. Methods **23**, 245 (1963).

[3] N. A. Dobrotin, E. V. Denisov, S. A. Dubrovina, D. V. Emeljanov, I. N. Fetisov, V. V. Guseva, N. E. Hromich, V. G. Ignatjeva, V. M. Kim, K. A. Kotelnikov, A. M. Lebedev, V. M. Maximemko, A. E. Morosov, A. G. Novikov, O. F. Ogurzov, V. S. Puchkov, D. F. Rakitin, S. A. Slavatinski, V. V. Sokolovsky, V. I. Titvo, and N. G. Zelevinskaya, in *Proceedings of the Ninth International Conference on Cosmic Rays, London, 1965* (The Institute of Physics and The Physical Society, London, 1966), Vol. 2, p. 817.

[4] E. W. Cowan and M. K. Moe, Rev. Sci. Instr. **38**, 874 (1967).

[5] L. W. Jones, in Proceedings of the Tenth International Conference on Cosmic Rays, Calgary, 1967, Part A, p. 480 (unpublished).

[6] K. Pinkau, U. Pollvogt, W. Schmidt, and R. W. Huggett, in *Proceedings of the Ninth International Conference on Cosmic Rays, London, 1965* (The Institute of Physics and The Physical Society, London, 1966), Vol. 2, p. 821.

[7] N. L. Grigorov, G. P. Kahidze, V. E. Nesterov, I. D. Rapoport, I. A. Savenko, A. V. Smirnov, A. I. Titenkov, and P. P. Shishkov, Cosmic Research **5**, 333 (1967).

[8] See, for example, K. Pinkau, Phil. Mag. **2**, 1389 (1957); and P. K. Malhotra, P. G. Shukla, S. A. Stephens, B. Vijaylakshmi, J. Boult, M. G. Bowler, P. H. Fowler, K. L. Hackforth, J. Keereetaveep, V. M. Mayes, and S. N. Tovey, Nuovo Cimento **40A**, 385 (1965).

[9] K. Pinkau and K. V. Thompson, Rev. Sci. Instr. **37**, 302 (1966).

[10] A. Somogyi, G. Valas, and A. Varga, Can. J. Phys. **46**, S1107 (1968).

[11] D. E. Lyon and A. Subramanian, MURA Report No. 725, 1967 (unpublished).

[12] W. V. Jones, K. Pinkau, U. Pollvogt, W. K. H. Schmidt, and R. W. Huggett, Nucl. Instr. Methods **72**, 173 (1969).

reliability of using such a device for energy measurements. In addition, Monte Carlo calculations can supply valuable information on modes of energy dissipation, e.g., nuclear disintegrations,[13] which are largely unsampled in most ionization spectrometers. Such calculations can also provide information on the fraction of the initial energy dissipated outside the boundaries of a spectrometer, since in the calculations the cascading particles can be followed to almost unlimited depths.

In this paper, a Monte Carlo method is reported for simulating the longitudinal development of a nuclear-electromagnetic cascade in an absorber. The details of the model used to describe the cascade are given in Sec. II, along with pertinent information about the Monte Carlo technique used. The calculations simulate as accurately as possible measurements made at the Brookhaven Alternating Gradient Synchrotron (AGS) with apparatus employing an iron-scintillator spectrometer. In Sec. III, the results of the calculations are compared with the AGS measurements, and the results of the calculations for higher energies are given.

II. CALCULATIONS

A. Cascade Model

In principle it should be possible to simulate exactly the nuclear-electromagnetic cascade process in any absorber. However, this process is extremely complicated and too little is presently known about the individual high-energy interactions spawning the cascade to make exact simulation possible. The most one can hope for is to be able to make use of available knowledge to predict the dominant over-all properties of the cascade development.

A search of the literature indicates rather widespread disagreements in regard to mean values and fluctuations of many parameters characterizing individual interactions. However, an attempt has been made to use the available experimental data to formulate a model which simulates reasonably well the actual nuclear-electromagnetic cascade. Because of the complexity of the problem, only the interaction characteristics which govern the dominant cascade growth have been considered. Fairly well-known data of various production and decay schemes of hadrons with heavy masses could be used to refine the model, but their inclusions is not expected to change the gross properties of the cascade development.

The calculations described herein are based on the following assumptions about the nuclear-electromagnetic cascade model:

(1) A single proton of known primary energy E_0 is incident on the spectrometer at the depth $t=0$.

(2) The proton interacts successively in the spectrometer at depths t governed by the probability distribution

$$g_N(t)dt=\lambda_N^{-1}e^{-t/\lambda_N}dt, \tag{1}$$

where t is measured in radiation lengths (r.l.), and λ_N ($\lambda_N=10.0$ for iron) is the number of radiation lengths per interaction length for proton interactions.

(3) Between interactions the proton loses the energy E_{ion} by ionization according to the relation

$$E_{\text{ion}}=\epsilon_0 t, \tag{2}$$

where ϵ_0 is the critical energy ($\epsilon_0=21$ MeV for iron) of the absorbing material.

(4) During the interaction of a proton of instantaneous energy E, the energy E_d goes into disintegration of the struck nucleus. The energy E_d is taken to follow the empirical relation[14,15]

$$\begin{aligned} E_d(\text{MeV})&=124N_h+30, \quad E>1 \text{ GeV} \\ &=37N_h+4N_h^2, \quad E\leq 1 \text{ GeV}. \end{aligned} \tag{3}$$

The parameter N_h is the number of heavily-ionizing nuclear evaporation fragments resulting from the interaction. The mean value of N_h is taken to follow the relations

$$\begin{aligned} \langle N_h\rangle&=3.46E^{1/6}A^{0.19}, \quad E>30 \text{ GeV} \\ &=2.1E^{1/3}A^{0.19}, \quad E\leq 30 \text{ GeV} \end{aligned} \tag{4}$$

where A is the atomic mass number of the absorbing material, and E is expressed in GeV. The power of E is based on considerations described in Ref. 14. The A dependence was chosen to be the same as that for secondary particle emission in the hydrodynamical model of Belenki and Landau for nucleon-nucleus collisions.[16] The distribution of N_h is taken to be a Poisson distribution.

(5) The inelasticity K of the interaction is chosen to follow the beta distribution

$$f(K)=\frac{\Gamma(\alpha+\beta+2)}{\Gamma(\alpha+1)\Gamma(\beta+1)}K^\alpha(1-K)^\beta. \tag{5}$$

This inelasticity is taken to be the fraction of the primary energy carried away from the interaction by secondary pions. The parameters α and β are chosen such that the mean value of the inelasticity $\langle K(A)\rangle$ for an absorber (taken to be 0.6 for iron) with atomic mass

[13] See, for example, V. S. Murzin, in *Progress in Elementary Particle and Cosmic Ray Physics*, edited by J. G. Wilson and S. A. Wouthhuysen (North-Holland Publishing Co., Amsterdam, 1967), Vol. 9, Chap. 4, p. 245.

[14] C. F. Powell, P. H. Fowler, and D. H. Perkins, *The Study of Elementary Particles by the Photographic Method* (Pergamon Press, Inc., New York, 1959), Chap. 13, p. 423.

[15] R. H. Brown, U. Camerini, P. H. Fowler, H. K. Heitler, D. T. King, and C. F. Powell, Phil. Mag. **40**, 862 (1949).

[16] S. Z. Belenkji and L. D. Landau, Nuovo Cimento Suppl. 3, 15 (1956).

number A is consistent with the relation[17,18]

$$\langle K(A)\rangle = 1-(1-\langle K_{n-n}\rangle)^{\phi}, \tag{6}$$

where K_{n-n} is the inelasticity for nucleon-nucleon collisions and

$$\phi = A^{1/3}. \tag{7}$$

The parameters α and β are related, respectively, to the mean and standard deviation of K by

$$\langle K\rangle = \frac{\alpha+1}{\alpha+\beta+2} \tag{8}$$

and

$$\sigma^2 = \frac{(\alpha+1)(\beta+1)}{(\alpha+\beta+2)^2(\alpha+\beta+3)}. \tag{9}$$

Therefore, with $\langle K\rangle$ fixed by Eq. (6) for a given absorber, one may choose one of the parameters α or β so that the spread of the K distribution is reasonable, say about 20–25% of the mean.

(6) The mean multiplicity $\langle N\rangle$ of secondary particles (taken here to be only pions) produced in each proton interaction follows the empirical formula

$$\begin{aligned}\langle N\rangle &= 1.86E^{1/4}A^{0.19}, \quad E>50 \text{ GeV}\\ &= 0.70E^{1/2}A^{1.19}, \quad E\leq 50 \text{ GeV}\end{aligned} \tag{10}$$

where, again, A is the atomic mass number of the absorbing material and E is the instantaneous energy (expressed in GeV) of the incident proton before the interaction. This equation is based on a combination of the results given by Malhotra[19] in his survey of the reported mean multiplicities for nucleon-nucleon interactions and the hydrodynamical model of Belenkji and Landau[16] which gives a mass dependence of $A^{0.19}$ for nucleon-nucleus collisions. The dependence appears to be consistent with measurements of $\langle N\rangle$ in emulsion for proton interactions.[20] Equation (10) should be interpreted as representing $\langle N\rangle$ for the forward cone in the laboratory system. It is only this forward cone which is important for the cascade development. It is assumed that N follows a Poisson distribution.

(7) The created pions share the fraction K (inelasticity) of the energy E available for pion production. The energy E' received by any particular pion is determined at random from the distribution[21]

$$f(E')dE' = T^{-1}e^{-E'/T}dE', \tag{11}$$

where

$$T = KE/N \tag{12}$$

is the average energy of the pions. These equations are used subject to the constraint that the sum of the energies of all pions created in an individual interaction must be equal to the energy KE. The energy $(1-K)E-E_d$ is carried away by the proton which retains its identity during the interaction.

(8) The charge of a created pion is chosen from a binomial distribution so that on the average $\frac{2}{3}$ of the pions are charged and $\frac{1}{3}$ are neutral. No difference between positive and negative pions is considered.

(9) Each created neutral pion decays instantaneously into two γ rays. The fraction of the neutral pion energy received by one of the γ rays is chosen at random from a uniform distribution. The other γ ray is assigned the remainder of the energy of the neutral pion. The γ rays undergo pair production at depths governed by the probability distribution

$$g_\gamma(t)dt = \lambda_\gamma^{-1}e^{-t/\lambda_\gamma}dt, \tag{13}$$

where λ_γ is one conversion length, which is equivalent to 9/7 r.l.[22] The energy of one electron from each γ ray is also chosen at random from a uniform distribution, while the other electron receives the remainder of the energy of the mother γ ray. Each of these electrons is in turn taken to form an independent electromagnetic cascade governed by approximation B of Rossi.[22] No fluctuations in the cascade development described by approximation B are considered.

(10) Each created charge pion interacts at depths determined from the probability distribution

$$g_\pi(t)dt = \lambda_\pi^{-1}e^{-t/\lambda_\pi}dt, \tag{14}$$

where λ_π ($\lambda_\pi = 11.9$ for iron) is the number of radiation lengths per interaction length for pion interactions in the absorber.

(11) The ionization energy loss along the paths of the charged pions is equivalent to that of protons having the same path length as given by Eq. (2). Furthermore, the nuclear disintegration energy in pion interactions is taken to be the same as that in the interaction of protons of the same energy. This is given by Eqs. (3) and (4).

After the interaction of a pion, no distinction is made between the incident pion and one of the created pions, i.e., the incident pion loses its identity in the collision. The term multiplicity for such interactions indicates the total number of pions emitted from the interaction. The mean of this number is considered to be slightly different than for proton interactions[19] and is taken to follow the relation

$$\begin{aligned}\langle N\rangle &= 1.83E^{1/4}A^{0.19}, \quad E>40 \text{ GeV}\\ &= 0.73E^{1/2}A^{0.19}, \quad E\leq 40 \text{ GeV}\end{aligned} \tag{15}$$

[17] S. A. Azimov, A. M. Abdullaev, V. M. Myalovsky, and T. S. Yuldashbaev, in *Proceedings of the 1963 Cosmic Ray Conference Jaipur, India*, edited by R. R. Daniel *et al.* (Commercial Printing Press, Ltd., Bombay, India, 1963), Vol. 5, p. 69.

[18] W. V. Jones, K. Pinkau, U. Pollvogt, W. K. H. Schmidt, and R. W. Huggett (unpublished).

[19] P. K. Malhotra, Nucl. Phys. **46**, 559 (1963).

[20] E. Lohrmann, M. W. Teucher, and M. Schein, Phys. Rev. **122**, 672 (1961).

[21] G. Cocconi, L. J. Koester, and D. H. Perkins, University of California Lawrence Radiation Laboratory Report No. UCID-1444, High Energy Physics Study Seminars No. 28 (Part 2), 1961 (unpublished).

[22] B. Rossi, *High Energy Particles* (Prentice-Hall, Inc., Englewood Cliffs, N. J., 1952).

where E is the instantaneous energy (expressed in GeV) of the pion before the interaction. It is assumed that N follows the Poisson distribution.

The energy available for particle production is shared among the produced pions. The energy E' of each pion is selected at random from the distribution

$$f'(E')dE' = T^{-1}e^{-E'/T}dE', \tag{16}$$

where

$$T = E/N \tag{17}$$

is the average pion energy. As in the case of proton interactions, this expression represents only the forward cone.

Some justification should be given here for using approximation B to convert the energy of the electromagnetic cascades to particle numbers (assumption 9). From a purely theoretical standpoint, this approximation cannot give the correct number of particles near zero energy.[22] However, for absorbers having a low atomic mass number, it is capable of yielding valid results on the number of electrons with energy not much smaller than the critical energy. The errors introduced in the solution of cascade theory by approximation B increase with atomic mass number to the extent that the results may not be reliable in heavy absorbers, even for electrons with energies greater than the critical energy. Nevertheless, approximation B offers the only consistent theoretical framework at very high energies for the electromagnetic cascade development. Furthermore, the approximation becomes increasingly realistic with increasing energy of the particle initiating the cascade. A recent investigation[23] has indicated that approximation B is sufficiently reliable for predicting the total number of particles in a cascade developing in nuclear emulsion ($A \approx 80$) for primary energies greater than about 100 GeV (which was the lowest energy studied in that investigation). Any errors arising from the use of approximation B in the calculations presented here are expected to be substantially less than natural fluctuations in the high-energy interaction parameters and/or errors introduced as a result of using a cascade model which does not take into account some of the finer details of the high-energy interactions.

B. Comparison of Monte Carlo Spectrometer with an Actual Spectrometer

The calculations have been performed for the geometrical configuration of an actual spectrometer used to study cosmic rays. The spectrometer was also exposed for calibration purposes to protons at the Brookhaven AGS. The results of the calibration exposure determined the response of the spectrometer at known machine energies, and this response can be used as a direct check of the reliability of the calculations. In turn, the calculations can be used to extrapolate the experimental calibration measurements to higher energies, i.e., determine the response of the spectrometer at cosmic-ray energies.

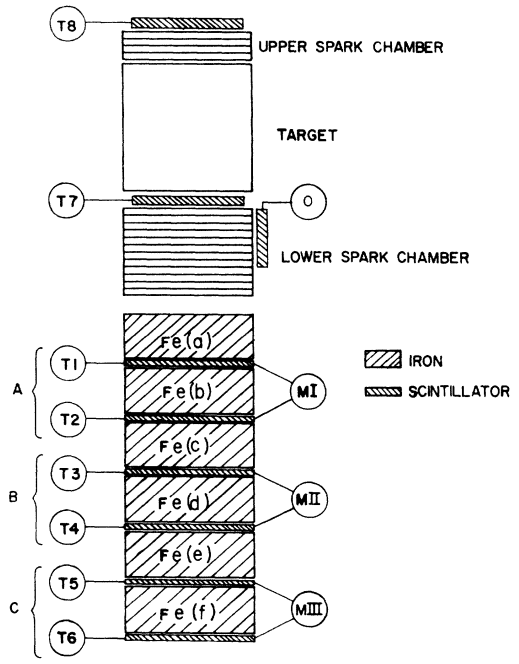

FIG. 1. Schematic diagram of the experimental apparatus used to make the measurements at the AGS (Ref. 18). The spectrometer is composed of six layers of iron each being ~4 r.l. thick and having a cross-sectional area of 18×18 cm². Six plastic scintillators are used as particle counters. Above the spectrometer are two spark chambers, a target material and two additional plastic scintillators. The top scintillator was used for charge measurements and as part of the trigger coincidence in balloon exposures of the apparatus. The scintillator directly under the target was used in conjunction with the lower spark chamber to identify events undergoing an interaction in the target.

A schematic diagram of the experimental apparatus used in the AGS exposures is shown in Fig. 1. It was divided into two parts—(i) the spark chambers above and below the target and (ii) the spectrometer. Details of the apparatus as well as conditions of the exposure can be found in Ref. 12.

The important features of the spectrometer from the standpoint of comparison with the calculations are the type of absorber, the number and spacing of the counters used to sample the cascade development, and the method used to locate the first interaction of an incident particle. The spectrometer was composed of six layers of iron. Each layer was about half the interaction length or 4 r.l. in thickness. Thin plastic scintillation detectors (1 cm) were placed between adjacent iron layers. One additional scintillator was placed underneath the bottom iron layer. The outputs of two scintillators were grouped together to form one counter. The resulting three counters are labeled MI, MII, and MIII in Fig. 1. Each of the three counters indicated the

[23] R. Holynski, W. V. Jones, and K. Pinkau, Phys. Rev. **176**, 1661 (1968).

TABLE I. Means and standard deviations of particle numbers predicted by the Monte Carlo calculations and the AGS measurements (in parentheses) for events with the first interaction in layer Fe(a) of the spectrometer.

E_0 (GeV)		N_1	N_2	N_3	N_{max}	$\sum N$
10	Mean	13.9 (12.7)	7.9 (4.7)	4.0 (2.4)	15.1 (13.5)	24.7 (19.1)
	Std. dev.	7.4 (6.7)	3.9 (4.4)	2.8 (3.1)	6.6 (6.5)	7.2 (8.0)
20.5	Mean	27.4 (22.9)	17.6 (13.1)	9.3 (5.9)	30.3 (26.1)	53.3 (41.6)
	Std. dev.	13.9 (12.9)	8.1 (9.4)	6.1 (6.8)	12.1 (11.7)	14.5 (15.5)
28	Mean	36.0 (30.4)	25.2 (18.8)	13.3 (9.0)	40.6 (35.5)	73.5 (58.1)
	Std. dev.	17.5 (17.6)	11.5 (12.3)	8.4 (9.0)	15.1 (15.2)	19.1 (20.0)
100	Mean	108.6	99.2	56.0	131.0	263
	Std. dev.	50.9	39.9	29.0	42.8	66
300	Mean	273	322	185	375	779
	Std. dev.	128	124	81	116	194
500	Mean	413	555	314	614	1281
	Std. dev.	195	199	131	184	309
1000	Mean	731	1138	661	1217	2530
	Std. dev.	342	390	254	351	592

average number of particles passing through the two corresponding scintillators whenever a particle was incident on the spectrometer. In addition, each scintillator was connected to two thresholds indicating, respectively, the passage of at least two or at least thirteen particles. These thresholds were used to locate the iron layer in which the first interaction of a single incident hadron had occurred. The spark chambers were used to determine whether or not a particle incident on the apparatus suffered an interaction in the target material.

The Monte Carlo spectrometer was designed to approximate as closely as possible the actual spectrometer used for the AGS measurements. The calculations have been made for single protons incident on an iron absorber with six Monte Carlo Counters being spaced every 4 r.l. The average number of particles in two adjacent counters is recorded separately in order to make direct comparisons with the experimentally measured distributions of particles in counters MI, MII, and MIII.

The calculations were performed for each proton incident on the spectrometer by following the proton and all the created secondary pions (as well as the additional pions created in all subsequent interactions) through successive interactions until they either passed through the bottom of the spectrometer or were stopped within the spectrometer. The number of particles in the electromagnetic component was determined from approximation B (assumption 9 of the cascade model), i.e., no attempt was made to follow individual particles in the electromagnetic cascade. The parameters governing each individual interaction were selected at random from the respective distributions given by the assumed cascade model.

The properties of the nuclear-electromagnetic cascade in the spectrometer which could be calculated by the computer program for each incident proton include: (i) the number of (a) proton and (b) pion interactions in each layer; (ii) the total number of particles in the cascade at each counter; (iii) the total number of particles in the cascade integrated over all consecutive counters; (iv) the number of particles at the maximum cascade development; (v) the layer in which the maximum cascade development occurs; (vi) the fraction of the incident energy passing through each counter in the form of (a) protons, (b) pions, (c) the electromagnetic cascade, and (d) protons, pions, and the electromagnetic cascade; (viii) the fraction of the incident energy going into nuclear disintegrations in each layer from (a) proton interactions, (b) pion interactions, and (c) proton and pion interactions.

The computer program could be run for arbitrarily many incident protons (2000 events were used), and, subsequently, the means and standard deviations for each of the cascade properties (i) through (vii) could be determined.

It should be noted that a major difference exists between the Monte Carlo calculations and the AGS measurements, since the calculations give information only on the longitudinal development of the cascades. Effectively, the Monte Carlo spectrometer has unlimited lateral dimensions while the spectrometer with which the calculations are compared had a cross-sectional area of 18×18 cm^2. Furthermore, in the AGS measurements events were accepted which were incident within an 8×8-cm^2 entrance area at the top of the apparatus. (See Fig. 1.) One can thus expect that a substantial number of the cascading particles will pass through the side walls of the spectrometer. Consequently, the agreement between the calculations and the measurements is not expected to be exact. Rather, a comparison of the observations with the one-dimensional simulation (which predicts the total number of particles in the cascade at various depths) can be used to determine the amount of energy passing through the sides of the spectrometer.

III. RESULTS AND COMPARISON WITH EXPERIMENTAL MEASUREMENTS

The analysis of the data taken at the AGS provided information on the distribution of the particle numbers N_1, N_2, and N_3 occurring, respectively, in counters MI, MII, and MIII. Other distributions were also derived from the distributions in the individual counters. These included mainly $\sum N=N_1+N_2+N_3$ and N_{max}, the maximum value of N_1, N_2, and N_3. The means and standard deviations of these distributions are given in Table I along with the corresponding results of the

Monte Carlo calculations. Also included are the results of the calculations for higher energies extending up to 1000 GeV. Table I is only for events which had the first interaction in the top layer Fe(a) of the spectrometer.

Comparisons of the measurements and the calculations at the AGS energies show that the means for the Monte Carlo distributions are consistently higher than those for the AGS distributions. This is to be expected, as mentioned in Sec. II B. In order to check the agreement of the calculations with the measurements, one should not rely too heavily on the means, but rather more emphasis should be placed on the shapes of the distributions. Furthermore, the number of particles occurring in the maximum of the cascade development, in conjunction with the depth in the spectrometer where the maximum occurs, should provide one of the best checks of the calculations. This is true, first of all, because the number of particles at the maximum is expected to have smaller statistical fluctuations than at any other position in the cascade and, secondly, because for agreement to exist, it is necessary that the positions of the maximum occur at the same depth in the spectrometer.

Figures 2 and 3 display, respectively, the distributions of particles at the maximum and the position of the maximum at 20.5-GeV primary energy. Inspection of

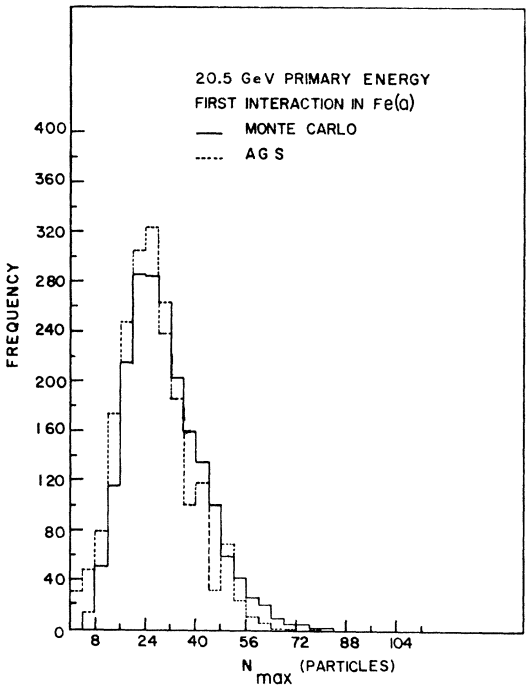

FIG. 2. Comparison of the number of events at the maximum of the cascade development at 20.5-GeV primary energy for the Monte Carlo calculations and the AGS measurements. The events considered are those which suffered the first interaction in layer Fe(a). The AGS events are normalized to 2000, the number of events used in the Monte Carlo calculations. The actual number of AGS events represented in 1679.

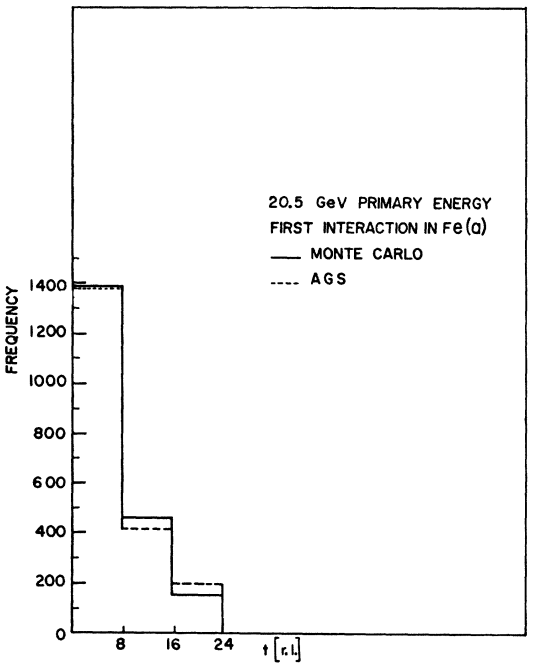

FIG. 3. Comparison of the number of events having the maximum number of particles occurring at depth t in the spectrometer for the Monte Carlo calculations and the AGS measurements. The events considered are those at 20.5 GeV primary energy having the first interaction in layer Fe(a). The AGS measurements are normalized to 2000 events, the number of events used in the Monte Carlo calculations. The actual number of AGS events represented is 1679. The histograms are given in intervals of 8 r.l., which was the smallest interval that could be determined for the AGS measurements. The heights of the three vertical bars in the histograms represent the number of events where the maximum of the cascade development occurred in N_1, N_2, and N_3 (i.e., in counters MI, MII, and MIII), respectively.

Fig. 2 shows that the calculated and measured distributions are quite similar. As expected, the calculated distribution is slightly shifted toward higher particle numbers. There is also rather good agreement in the position where the maximum occurs, as can be seen from Fig. 3. This latter check is admittedly quite crude, since one can only check in which one of the three spectrometer counters (representing intervals of 8 r.l.) the maximum development occurred.

Distributions of $N_{\max}$ and the position of $N_{\max}$ at 10 and 28 GeV are analogous to the examples given for 20.5 GeV. The actual shift in the mean of $N_{\max}$ is larger at 28 GeV and smaller at 10 GeV. However, the relative displacement decreases with energy.

It was concluded from analysis of the AGS data that $\sum N$ was the parameter with the narrowest distribution for a given primary energy and, therefore, was best suited for determining the unknown energy of a particle incident on the spectrometer.[12] Consequently, this is perhaps the most interesting parameter for comparison of the Monte Carlo calculations with experimental results. The comparison is shown in Figs. 4(a)–4(c) for events having the first interaction in

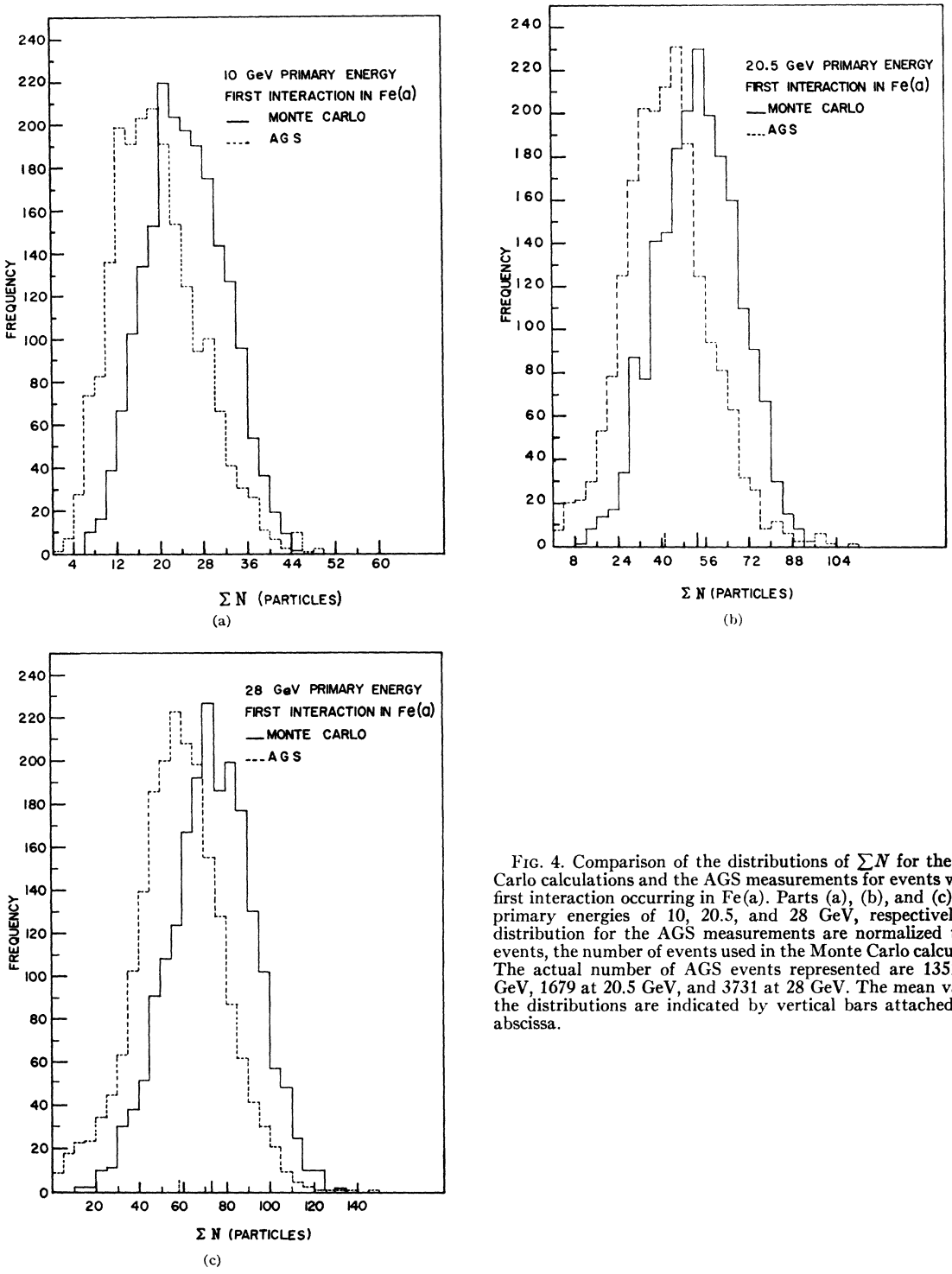

FIG. 4. Comparison of the distributions of $\sum N$ for the Monte Carlo calculations and the AGS measurements for events with the first interaction occurring in Fe(a). Parts (a), (b), and (c) are for primary energies of 10, 20.5, and 28 GeV, respectively. The distribution for the AGS measurements are normalized to 2000 events, the number of events used in the Monte Carlo calculations. The actual number of AGS events represented are 1351 at 10 GeV, 1679 at 20.5 GeV, and 3731 at 28 GeV. The mean values of the distributions are indicated by vertical bars attached to the abscissa.

layer Fe(a) at all three AGS energies. The experimental and calculated distributions appear to be quite similar except for the expected scale shift. The relatively few AGS events having larger values of $\sum N$ than ever predicted by the calculations may be attributed to fluctuations in the electromagnetic-cascade development and/or to ionization bursts occurring in the scintillators, neither of which was taken into account in the calculations.

The agreement of the shapes of the $\sum N$ distributions

when plotted in equal intervals of $\sum N$ (in conjunction with the displaced mean) implies that the experimental $\sum N/\langle\sum N\rangle$ distributions are actually wider than the calculated ones. The extent of the difference in shape in the latter distributions is indicated in Fig. 5, where the distributions at 28-GeV primary energy are plotted in equal increments of $\sum N/\langle\sum N\rangle$. The situation is analogous at 10 and 20.5 GeV.

All of the results discussed thus far have been for events which suffered the first interaction in layer Fe(a) of the spectrometer. Calculations have also been performed for incident protons without any restriction as to where the first interaction occurred. These latter calculations can also be compared with measurements from the AGS exposures. Qualitatively, the agreement (or difference) follows the same patterns (shift in the mean, etc.) that have already been established for events having the first interaction in Fe(a). In general, the distributions are somewhat wider if the position of the first interaction is not restricted. Furthermore, each distribution has a characteristic peak corresponding to the depth in the spectrometer penetrated by an incident particle before it interacted.

An example of the results for all incident events (regardless of the position of first interaction) is given in Fig. 6. The distribution is for $\sum N$ at 28-GeV primary energy. The characteristic peak in the intevral $0 \leq \sum N < 5$ particles results from the relatively large number of events which penetrated the entire spectrometer without interacting, so that $\sum N = 3$. This characteristic peak is somewhat higher for the calculations than for the AGS measurements. Furthermore, the calculated distribution, apart from having the expected displacement in the mean, is significantly wider than the measured one.

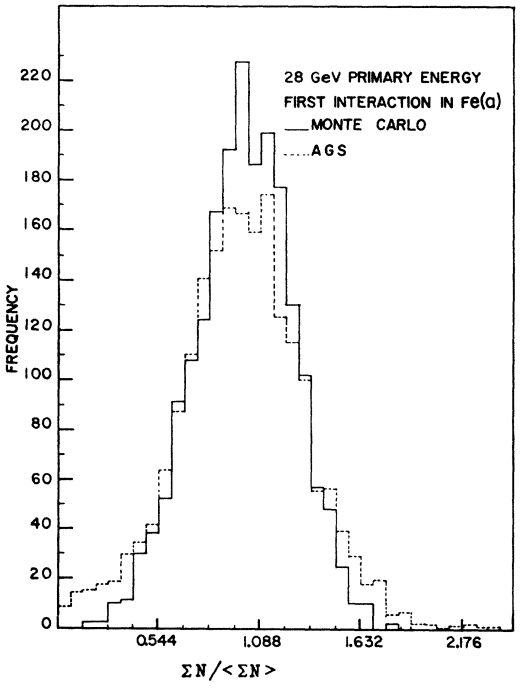

FIG. 5. Comparison at 28-GeV primary energy of the distributions of $\sum N/\langle\sum N\rangle$ for the Monte Carlo calculations and the AGS measurements for events with the first interaction occurring in layer Fe(a). The 3731 AGS measurements are normalized to 2000 events, the number of events used in the calculations.

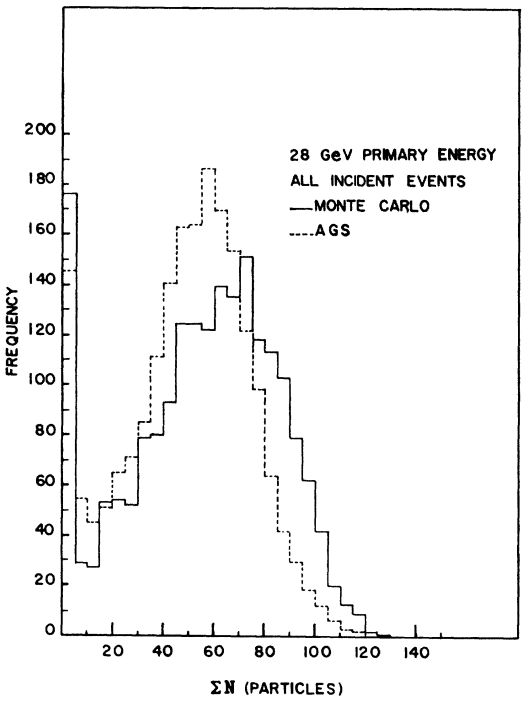

FIG. 6. Comparison of $\sum N$ for Monte Carlo calculations and AGS measurements at 28-GeV primary energy for all events incident on the spectrometer, regardless of the depth of the first interaction. The AGS measurements represent 3519 events normalized to 2000, the number of events used in the calculations.

These two effects are related, and both of them can be directly attributed to deficiency of the experimental apparatus for detecting all of the interactions occurring above the spectrometer. (The problems involved in locating the first interaction of particles incident on the apparatus are discussed in detail in Ref. 18). The AGS events listed as being single protons incident on the spectrometer are actually contaminated with events which had undergone at least one interaction in the target and/or in the spark chamber and mounting materials above the spectrometer. This contamination will, of course, result in appreciable narrowing of the distributions and in reducing the fraction of the events having $\sum N = 3$. The contamination depends, among other things, on the type of material used in the target, and it is believed to range from 10–30%.

In Fig. 7, the AGS distribution shown in Fig. 6 is compared with Monte Carlo predictions for all incident events subject to the constraint that 20% of the events were chosen at random to interact at the

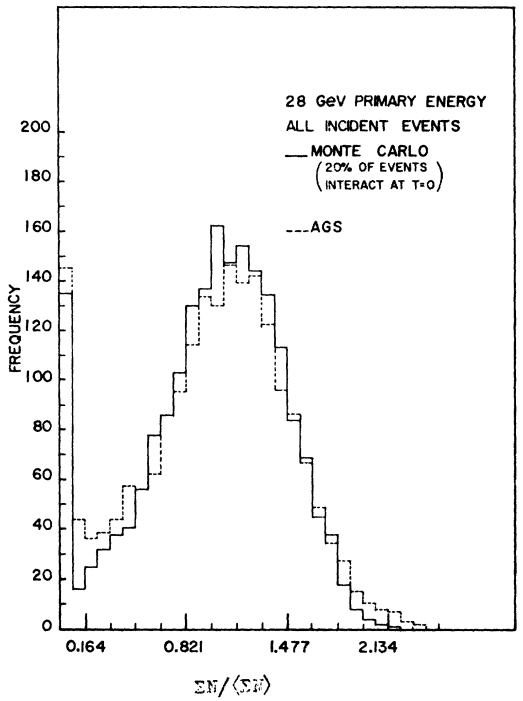

FIG. 7. Comparison of $\sum N/\langle\sum N\rangle$ for the Monte Carlo calculations and AGS measurements at 28-GeV primary energy for all events incident on the spectrometer, regardless of the depth of the first interaction. For the Monte Carlo calculations, 20% of the events were selected at random to interact at the upper boundary (depth $t=0$) of the spectrometer. The AGS measurements represent 3519 events normalized to 2000, the number of events used in the calculations.

upper boundary of the spectrometer. The distribution is plotted in equal increments of $\sum N/\langle\sum N\rangle$ to show the shapes of the distributions about the mean. Although somewhat synthetic, the agreement is quite good, including the slightly narrower calculated distribution which has already been attributed to neglecting electromagnetic cascade fluctuations.

TABLE II. Means and standard deviations of the energy not deposited in depth t of the spectrometer; given in percent of the primary energy E_0 for events with the first interaction in layer Fe(a).

t (r.l.)	E_0 (GeV)	10	20.5	28	100	300	500	1000
4	Mean	79.2	86.0	88.5	94.8	97.3	98.0	98.5
	Std. dev.	9.4	6.4	5.5	3.1	2.0	1.4	0.1
8	Mean	59.0	67.8	71.6	81.7	87.4	89.4	91.4
	Std. dev.	15.2	12.0	11.0	7.8	6.1	5.3	4.4
12	Mean	42.5	51.3	55.2	66.5	73.3	75.8	78.6
	Std. dev.	17.5	15.1	14.1	11.4	9.6	8.6	7.6
16	Mean	31.3	41.0	43.9	55.3	62.0	64.6	67.4
	Std. dev.	17.3	15.8	15.0	13.1	11.7	10.7	9.8
20	Mean	23.4	31.5	35.5	46.6	53.4	55.9	58.7
	Std. dev.	16.0	15.4	14.9	13.6	12.5	11.7	10.8
24	Mean	17.5	25.0	28.6	39.2	46.0	48.7	51.5
	Std. dev.	14.2	14.2	14.4	13.4	12.6	11.9	11.1

TABLE III. Means and standard deviations of the energy going into nuclear disintegrations within depth t of the spectrometer; given in percent of the primary energy E_0 for events with the first interaction in layer Fe(a).

t (r.l.)	E_0 (GeV)	10	20.5	28	100	300	500	1000
4	Mean	16.8	10.9	8.8	3.5	1.7	1.3	1.0
	Std. dev.	7.5	4.8	3.9	1.9	1.1	0.7	0.3
8	Mean	24.1	16.6	13.7	6.8	3.7	2.8	1.9
	Std. dev.	10.6	7.2	6.0	3.0	1.8	1.4	1.1
12	Mean	29.9	21.5	18.3	9.9	5.9	4.7	3.4
	Std. dev.	11.8	8.5	7.0	4.0	2.5	1.9	1.5
16	Mean	34.7	25.6	22.1	12.9	8.1	6.6	5.0
	Std. dev.	12.3	9.3	7.8	4.7	3.0	2.5	1.8
20	Mean	38.2	29.2	25.2	15.7	1.0	8.6	6.7
	Std. dev.	12.3	9.6	8.4	5.3	8.5	2.9	2.2
24	Mean	41.7	32.3	28.5	18.3	12.6	10.5	8.4
	Std. dev.	11.9	9.6	8.7	5.7	3.9	3.3	2.5

Distributions of $\sum N$ at 500-GeV primary energy are given in Fig. 8 as an example for the higher energies which have been calculated. A qualitative comparison of this figure with Figs. 4 and 6 shows that regardless of whether one considers all incident events or only events which have the first interaction in Fe(a), the shapes of the distributions exhibit no significant change with primary energy. This is, of course, a desirable feature of the cascade development when using an ionization spectrometer for the determination of unknown energies.

The predictions of the calculations for the means and standard deviations of the energy not deposited within given depths of the spectrometer are given in Table II for events having the first interaction in Fe(a). It can be seen from the table that the fraction of the primary energy leaking beyond a given layer decreases with increasing depth of the layer in the spectrometer and increases with primary energy.

In Table III, the mean and standard deviations predicted for the amount of energy dissipated within the spectrometer in the form of nuclear disintegrations are presented for the same primary energies and depths considered in Table II. The fraction of the primary energy going into nuclear disintegrations increases with depth of the spectrometer and decreases with increasing primary energy.

Since the energy dissipated in the form of nuclear disintegrations is for the most part unsampled by an ionization spectrometer, it can be combined with the energy leaking out the bottom of the spectrometer to give the total unmeasured energy loss for incident particles. Figure 9 displays, as a function of primary energy, the mean values of the percent of the primary energy leaking out the bottom ($t=24$ r.l.) of the spectrometer (E_{out}) and going into nuclear disintegration (E_d). Also included is the total unmeasured energy loss ($E_{\text{out}}+E_d$). For this shallow spectrometer, the unmeasured energy loss is fairly independent of energy over the range 10–1000 GeV.

In Ref. 12 the total amount of energy E_{ion} dissipated within the spectrometer for each of the three energies 10, 20.5, and 28 GeV was estimated by assuming a constant differential ionization energy loss along the path of the average cascade. The value of E_{ion} was determined from the expression

$$E_{\text{ion}}(\text{MeV}) = (N_1 + N_2 + 0.75N_3) \times 8 \times 21. \quad (18)$$

The factor 21 is the critical energy of iron in MeV. The factor 8 is the effective path length in radiation lengths represented by each of the measuring units from which the particle numbers N_1, N_2, and N_3 were obtained. The factor 0.75 enters because the lower scintillator of the third measuring unit constituted the lower edge of the spectrometer.

The same approach can be used as an additional check on the validity of Monte Carlo calculations. Since the total energy of a particle incident on the spectrometer is eventually completely dissipated either inside or outside the spectrometer boundaries, the sum of the percentages of the energy dissipated inside and outside must add up to 100% of the incident energy.

The average total energy passing below the spectrometer for events interacting in Fe(a) can be obtained from Table II. The average total energy dissipated within the spectrometer is the sum of the nuclear disintegration energy given in Table III and the energy dissipation of the average cascade, which can be calculated from Table I and Eq. (18). The results of the calculations for the different modes of energy dissipation are given in Table IV. For comparison, numerical results for the AGS measurements for E_{ion} [calculated from Table I and Eq. (18)] and E_{total} are also given in parentheses. (E_{total} means the measured value of E_{ion} added to the calculated values of E_{out} and E_d.)

Table IV shows that the different modes of energy dissipation predicted by the Monte Carlo calculations do indeed add up to 100% of the total energy. [The slight deviation about 100% is due to normal fluctuations that result from the use of Eq. (18) to calculate E_{ion}.] However, when the AGS measurements for the average energy dissipated within the spectrometer are added to the calculated nuclear disintegration energy and energy leaking out the bottom, the total energy dissipation amounts to about 91% of the incident energy. The 9% missing energy can be attributed to energy loss out the sides of the spectrometer.

It should be noted here that many changes were made in the parameters of the cascade model while doing the calculations in an attempt to get the means of the individual particle distributions into better agreement with the measured results. These changes included using several trial values for the interaction length and for the multiplicity, inelasticity, and number of nuclear evaporation fragments in individual interactions. Different values of these parameters affect, of course, the rate of growth and decay of the cascade, as well as its magnitude and fluctuations. It is not intended that these trial calculations be discussed in detail here. However, it can be stated that, in general, the cascade grows and decays more rapidly and the particle number distributions become more narrow for shorter interaction lengths, higher multiplicities, larger inelasticities, and for an increasing number of nuclear evaporation fragments. The cascade development appears to be especially sensitive to changes in the multiplicity.

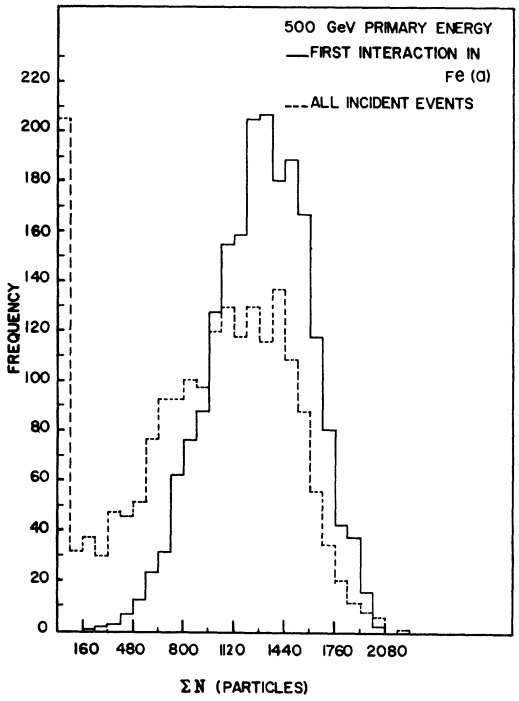

FIG. 8. Distributions of $\sum N$ predicted by the Monte Carlo calculations at 500-GeV primary energy for all events incident on the spectrometer, regardless of the depth of the first interaction, and for events having the first interaction in layer Fe(a).

It is interesting that, for any given incident energy, the sum of E_{out} and E_d varied only slightly, except when extreme values of the interaction parameters were used. However, moderate changes in the inter-

TABLE IV. Modes of energy dissipation in % of the primary energy E_0 for events with the first interaction in layer Fe(a) of the spectrometer. Results for the AGS measurements are given in parentheses.

E_0 (GeV)	E_{ion}	E_{out}	E_d	E_{total}
10	41.5 (32.0)	17.5	41.7	100.7 (91.2)
20.5	42.6 (33.0)	25.0	32.3	99.9 (90.3)
28	42.7 (33.6)	28.6	28.5	99.8 (90.7)
100	42.0	39.2	18.3	99.5
300	41.1	46.0	12.6	99.7
500	40.4	48.7	10.5	99.6
1000	39.7	51.5	8.4	99.6

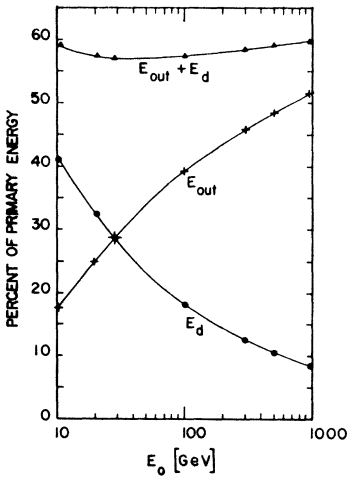

FIG. 9. The percentage of the primary energy E_0 leaking out of the bottom of the spectrometer (E_{out}), the percentage of E_0 going into nuclear disintegrations within the spectrometer (E_d), and the percentage of E_0 not measured by the spectrometer ($E_{out}+E_d$) plotted as a function of E_0.

action parameters resulted in appreciable variations in the sum of E_{ion}, E_{out}, and E_d. This latter sum was always significantly less than 100% of the incident energy whenever the calculated value of E_{ion} approached the measured value, i.e., whenever the means of the calculated particle number distributions approached the means of the measured distributions. This fact substantiates the foregoing conclusion that an appreciable fraction of the incident energy was being lost out of the sides of the spectrometer in the AGS measurements.

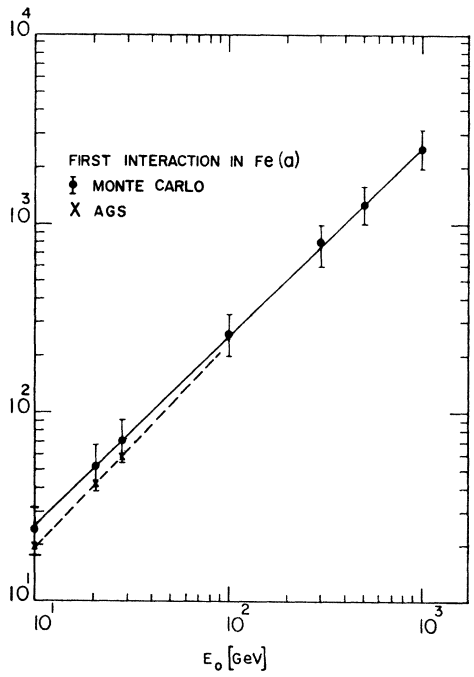

FIG. 10. The dependence of $\langle\sum N\rangle$ on primary E_0 predicted by the Monte Carlo calculations for proton events having the first interaction in layer Fe(a). The solid dots connected by the solid line represent the mean values of $\sum N$. The error bars indicate one standard deviation of the $\sum N$ distribution. The mean values of $\sum N$ for the AGS measurements are given by the crosses connected by the broken line. This line has been extrapolated beyond the largest measured energy value of 28 GeV.

IV. DISCUSSION

The comparisons of the calculated and measured particle distributions in Sec. III indicate that the Monte Carlo method used here does indeed provide a reasonable simulation of the nuclear-electromagnetic cascade development in the longitudinal direction. The only obvious difference between the AGS measurements and the calculations is the relative shift in the mean values of the various distributions. Arugments have been given to explain this effect in terms of particle leakage out of the sides of the spectrometer used for the measurements.

Additional evidence has been given which indicates that, on the average, the magnitude of the side-leakage amounts to about 9% of the incident energy for 10- to 28-GeV events interacting in the to player. If the position of the first interaction is unrestricted the side-leakage decreases to about 6–7%. This decrease results to a large extent from the appreciable number of events (~9%) which penetrated the entire depth of the spectrometer (24 r.l.) without interacting—thereby losing almost 100% of their energy out of the bottom and none out of the sides.

It has also been shown in Sec. III that the total unmeasured energy dissipation for the shallow spectrometer is fairly independent of primary energy. Besides the side leakage, Fig. 9 indicates that in the primary energy range between 10–1000 GeV about 55–60% of the primary energy cannot be measured by the spectrometer. It should be noted, however, that for similar spectrometer designs but of sufficiently large depth, the energy leaking out of the bottom will become negligible for all energies. On the other hand, the nuclear disintegration energy will continually increase with depth until it approaches a constant value, depending on the primary energy, when no more interactions occur. This constant value, i.e., the total fraction of the incident energy going into nuclear disintegrations, represents the minimum unmeasured energy loss attainable for spectrometer designs which do not measure the disintegration energy.

It is not necessary that an ionization spectrometer measure all modes of energy dissipation in order for the spectrometer to be a useful device for determining the unknown energies of particles incident upon it. It is only necessary that the relationship with energy of some parameter characterizing the cascade development be established. The accuracy of the energy determination will, of course, depend on the fluctuations of that parameter at a given incident energy. It has been shown

in Ref. 12 that the parameter which gives the smallest fluctuations for the spectrometer considered here was $\sum N$. This is also borne out by the Monte Carlo calculations.

In Fig. 10 are plotted the mean values of $\sum N$ as a function of primary energy for both the AGS measurements and the calculations. The figure is for incident proton events which suffer the first interaction in layer Fe(a) of the spectrometer. The calculations show that $\langle \sum N \rangle$ is linearly dependent on the primary energy E_0 over the energy range 10–1000 GeV. The fluctuations to be expected at the calculated energies are indicated by error bars, which represent one standard deviation of the $\sum N$ distribution.

The AGS measurements appear not to be a linear function of energy, but rather to be dependent on a power law of energy with an exponent slightly larger than 1. This deviation from a truly linear dependence can be attributed to an increased loss of particles out the sides of the spectrometer for the lower primary energies. In fact, if one extrapolates the AGS measurements to higher energies, it is seen that at approximately 200 GeV the calculations and the measurements predict the same number of particles. This can be interpreted as meaning that at ~200 GeV the cascades are collimated sufficiently well so that a negligible loss of particles occurs through the sides of the spectrometer.

The accuracy with which the unknown energy of incident protons interacting in the top layer of the spectrometer can be determined from measurements of $\sum N$ is shown in Fig. 11. The values of ΔE are the limits of error in the energy determination corresponding to one standard deviation in the distribution of $\sum N$. The errors in the energy estimation for the AGS results are significantly larger than the errors predicted by the Monte Carlo calculations. However, the AGS errors appear to be converging to the Monte Carlo predictions as the energy increases. Therefore, the curves drawn through the AGS error points have been extrapolated to approach the calculated curves at ~200 GeV, where leakage of particles through the sides of the spectrometer is expected to be become negligible.

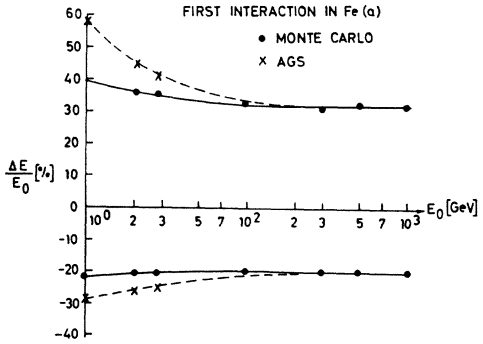

FIG. 11. The energy error $\Delta E/E_0$ as a function of the primary energy E_0. This is the error to be expected when $\sum N$ is used to estimate the unknown energy of incident protons having the first interaction in the top layer Fe(a) of the spectrometer. The energy error ΔE corresponds to one standard deviation in the distribution of $\sum N$ at the primary energy E_0. The dashed curve drawn through the AGS points has been extrapolated to approach at ~200 GeV the solid curve drawn through the points predicted by the Monte Carlo calculations.

Although not shown here, the parameter $\langle \sum N \rangle$ for events not restricted to having the first interaction in layer Fe(a) has a power-law dependence on primary energy with an exponent slightly less than one (~0.97). The relations between the calculations and the AGS measurements for these events are analogous to those shown in Figs. 10 and 11 for interactions occurring in Fe(a).

ACKNOWLEDGMENTS

The author wishes to express his appreciation to the staffs of the Computer Research Centers of the Max Planck Institut and of Louisiana State University for the use of their IBM 360/50 and IBM 360/65 computers, respectively. He would like to thank R. W. Huggett, K. Pinkau, U. Pollvogt, and W. K. H. Schmidt for permission to use the results of the AGS exposures of the ionization spectrometer. He is also grateful for the assistance of Mrs. Susan Garrett in doing numerical calculations and preparing numerous graphs.